Published in final edited form as:
*Osteoarthritis Cartilage*. 2014 October ; 22(10): 1724–1731. doi:10.1016/j.joca.2014.06.021.

# Quantification of differences in bone texture from plain radiographs in knees with and without osteoarthritis

**J. Hirvasniemi**[1,2], **J. Thevenot**[1,2], **V. Immonen**[1], **T. Liikavainio**[3], **P. Pulkkinen**[1,2], **T. Jämsä**[1,2,4], **J. Arokoski**[5,6], and **S. Saarakkala**[1,2,4]

[1]Department of Medical Technology, University of Oulu, Oulu, Finland [2]Medical Research Center Oulu, Oulu University Hospital and University of Oulu, Oulu, Finland [3]Muonio Health Centre, Muonio, Finland [4]Department of Diagnostic Radiology, Oulu University Hospital, Oulu, Finland [5]Institute of Clinical Medicine, University of Eastern Finland, Kuopio, Finland [6]Department of Physical and Rehabilitation Medicine, Kuopio University Hospital, Kuopio, Finland

## Abstract

**Objective—**To quantify differences in bone texture between subjects with different stages of knee osteoarthritis (OA) and age- and gender-matched controls from plain radiographs using advanced image analysis methods.

**Design—**Altogether 203 knees were imaged using constant X-ray parameters and graded according to Kellgren–Lawrence (KL) grading scale (KL0: $n$=110, KL1: $n$=28, KL2: $n$=27, KL3: $n$=31, KL4: $n$=7). Bone density-related and structure-related parameters were calculated from medial and lateral tibial subchondral bone plate and trabecular bone and from femur. Density-related parameters were derived from grayscale values and structure-related parameters from Laplacian- and local binary patterns (LBP)-based images.

**Results—**Reproducibilities of structure-related parameters were better than bone density-related parameters. Bone density-related parameters were significantly ($p$<0.05) higher in KL2-4 groups than in control group (KL0) in medial tibial subchondral bone plate and trabecular bone. LBP-based structure parameters differed significantly between KL0 and KL2-4 groups in medial subchondral bone plate, between KL0 and KL1-4 groups in medial and lateral trabecular bone,

Address correspondence and reprint requests to: Jukka Hirvasniemi, Department of Medical Technology, Institute of Biomedicine, University of Oulu, POB 5000, FI-90014 Oulu, Finland. Tel.: +358 294 48 6004. jukka.hirvasniemi@oulu.fi.
J. Thevenot: jerome.thevenot@oulu.fi
V. Immonen: ville.immonen2@gmail.com
T. Liikavainio: tuomas.liikavainio@muonio.fi
P. Pulkkinen: pasi.pulkkinen@oulu.fi
T. Jämsä: timo.jamsa@oulu.fi
J. Arokoski: jari.arokoski@kuh.fi
S. Saarakkala: simo.saarakkala@oulu.fi

**Author contributions**

Conception and design: JH, SS; acquisition of data: JH, JT (reproducibility analysis), VI (reproducibility analysis), TL, JA; analysis and interpretation of the data: all authors; drafting of the article: JH, SS; critical revision of the article for important intellectual content: JT, VI, PP, TJ, TL, JA, SS; final approval of the article: all authors.

**Conflict of interest**

The authors report no conflicts of interests.


Europe PMC Funders Author Manuscripts

and between KL0 and KL1-4/KL2-4 in medial and lateral femur. Laplacian-based parameters differed significantly between KL0 and KL2-4 groups in medial side regions-of-interest (ROIs).

**Conclusions—**Our results indicate that the changes in bone texture in knee OA can be quantitatively evaluated from plain radiographs using advanced image analysis. Based on the results, increased bone density can be directly estimated if the X-ray imaging conditions are constant between patients. However, structural analysis of bone was more reproducible than direct evaluation of grayscale values, and is therefore better suited for quantitative analysis when imaging conditions are variable.

**Keywords**

Radiography; osteoarthritis; bone; texture analysis; knee

## 1. Introduction

Osteoarthritis (OA) causes progressive degeneration of articular cartilage and abnormal changes in subchondral bone. Typical OA changes in the subchondral bone include thickening (sclerosis) as well as formation of osteophytes and subchondral bone cysts[1]. The actual definition of the extent of the subchondral bone varies, but it can be divided to the subchondral bone plate, located immediately beneath the calcified cartilage layer, and to the subchondral trabecular bone located beneath the subchondral bone plate[2-4].

Complete cure of OA does not currently exist, but the progression of the disease could be hindered if the diagnosis is confirmed at an early stage of the disease. Clinical diagnosis of OA is routinely based on clinical examination and changes on plain radiographs. Radiography is cheap, fast, and widely-available imaging modality. Articular cartilage is not visible on plain radiographs but OA changes including joint space narrowing, subchondral bone sclerosis and cysts, and osteophytes, can still be diagnosed[5]. Kellgren-Lawrence (KL) grading scale[6] is typically used for grading of OA from plain radiographs. However, KL grading is subjective, semi-quantitative, and according to the literature its intra- and inter-rater reliability varies from only moderate to substantial[7-9]. The diagnostic value of simple plain radiography could be enhanced if new quantitative and user-independent image analysis algorithms are developed and applied.

In earlier studies, quantitative evaluation of knee radiographs in OA have typically concentrated on the measurement of joint space width (JSW)[10, 11]. Some studies have calculated an estimate for bone density from plain radiographs[12, 13]. However, image acquisition parameters and post-processing algorithms significantly affect the density estimates[13]. In addition to JSW and density estimation, texture analysis is a potential method to extract quantitative and user-independent information of bony structures from plain radiographs. Texture analysis of bone is not as dependent on the imaging conditions as direct evaluation of grayscale values. In recent texture analysis studies, progression of OA has been evaluated from standard digital knee radiography using signature dissimilarity measure (SDM) method[14] and fractal signature analysis (FSA)[15]. Previously, fractal-based algorithms have been also applied for macro-radiographs[16-20] and standard film radiographs[20-23] from OA knees. The potential of gradient- or Laplacian-based image




Europe PMC Funders Author Manuscripts

processing algorithms that have already shown their effectiveness in hip fracture studies[24, 25], have not been studied in OA radiographs yet.

Another potential technique for the texture analysis of bone is local binary patterns (LBP) method that has been widely used in machine vision field[26]. It is simple and quite insensitive to monotonic grayscale variations, *e.g.*, in X-ray images to changes in radiation intensity (quantity of charge, so called mAs value). One dimensional LBP method has recently been applied in the trabecular bone analysis from the calcaneus[27]. However, LBP analysis from knee involving calculation of the texture parameters from LBP-based image might reveal more important information on bone structure.

The aim of the current study is to quantify differences in bone density and structure between subjects with different stages of knee OA and controls from plain radiographs using advanced image analysis methods. We hypothesize that simple grayscale parameters estimating subchondral bone density and quantitative bone structure-related texture parameters derived from Laplacian- and LBP-based images would be different among OA patients than among age- and gender-matched controls.

## 2. Methods

### 2.1. Study subjects

This study consisted of male patients ($n$ = 53, mean age (standard deviation (SD)): 59.4 (5.2) years, body mass index (BMI): 30.5 (4.7) kg/m$^2$) with unilateral or bilateral knee OA and healthy age-matched male controls ($n$ = 50, age: 59.5 (4.4) years, BMI: 27.8 (3.2) kg/m$^2$). From the original study population ($n$ = 107)[28, 29], four patients were excluded due to missing or different resolution of radiograph. Exclusion criteria included previous hip or knee fracture, surgery of lower extremities (arthroscopy was allowed), clinical or radiological hip OA, a knee or hip joint infection, congenital or developmental disease of lower limbs, paralysis of lower extremities, and rheumatoid arthritis or spondyloarthritis. The detailed exclusion criteria has been published earlier[28, 29]. The Ethics Committee of the Kuopio University Hospital approved the study design.

### 2.2. Acquisition of plain radiographs and grading of the knees

Anterior-posterior weight bearing radiographs from both knees were obtained using computed radiography (full extension, constant X-ray parameters: tube voltage = 60 kV, quantity of charge = 25 mAs, focus-skin distance = 110 cm) and digitized with a pixel resolution of 0.2 mm x 0.2 mm. The knees were classified according to the KL grading scale[6], in which 0 is normal and 4 is severe OA. KL grades were not known during the quantitative image analyses. In three knees, lateral side was more affected than the medial side and these knees were excluded from the analyses (one knee had KL grade 3 and two knees KL grade 4) to homogenize the study sample.

Both knees of the subjects (total number of samples = 203) were analyzed using custom-made MATLAB software (v.7.9.0; MathWorks Inc., Natick, MA, USA). First, the radiographs were converted to 8-bit grayscale images (pixel intensity value range: 0-255) and pixel size in the image was calibrated using a calibration ball with a diameter of 30 mm

included in each radiograph. Medial and lateral JSWs and minimum JSWs (mJSW) were measured manually from the middle part of the condyles and from the narrowest point of the joint (Figure 1), respectively.

### 2.3. Selection of regions-of-interest (ROIs)

Altogether six rectangle-shaped ROIs were extracted from the tibia and femur and one elliptical-shaped ROI (variable size) from the soft tissue beside the joint (Figure 1). Two ROIs (size: 70×30 pixels) were placed into the subchondral bone plate in the center of medial and lateral condyles of tibia, two ROIs (70×70 pixels) immediately below the subchondral bone plate in the subchondral trabecular bone in tibia, and two ROIs in the medial (70×70 pixels) and lateral condyles of femur (70×30 pixels). Smaller size of the lateral femur ROI was selected to avoid summation of the patella in the ROI. Anatomical landmarks for the tibial ROIs were tibial spine, subchondral bone plate, and outer borders of the proximal tibia. The center point of a condyle was first checked visually and was about half of the horizontal distance between the outer border of tibia and a vertical line drawn from the medial or lateral tibial spine. Subchondral trabecular bone ROIs were aligned horizontally with subchondral bone plate ROIs. However, some ROIs were moved towards the center of the tibia to avoid an overlapping with the fibula. Landmarks for the femoral ROIs were intercondylar notch of femur, subchondral bone plate, and outer borders of the distal femur. When placing femur ROIs, horizontal alignment of subchondral bone plate ROIs, plateau in the middle part of femoral condyles, and an overlapping with the patella were considered. The distance of the femur ROIs from the outer border of femur was typically about 1/4 of the horizontal distance from intercondylar notch of femur to the outer border of femur. Some ROIs were excluded due to distractions (*e.g.*, bright edges) from a piece of the clothing or similar artifact. The number of the tibial subchondral bone plate and trabecular bone ROIs and femur ROIs are shown in Tables 2, 3, and 4, respectively.

### 2.4. Evaluation of bone density

From unprocessed ROIs, mean grayscale value (GV), mean grayscale value of the soft tissue ROI subtracted from GV (=GV'), and GV divided by the depth of the tibia (=$GV_{norm}$) were calculated to estimate bone density. Tibia depth was empirically tested to be 0.72 (SD: 0.03) times tibia width in this dataset. This ratio was obtained by measuring the width of the tibia about 1 cm below the cartilage-bone interface from the anterior-posterior and lateral radiographs, which were also available for the study subjects. $GV_{norm}$ was not calculated for the femur ROIs since the depth of the femur would have been too difficult to reliably estimate from the correct location due to the curved shape of the femur.

### 2.5. Texture analysis of bone

From the ROIs, LBP[26] and second order partial derivatives (Laplacians) were calculated to construct LBP- and Laplacian-based images (Figure 2). Furthermore, an LBP-based contrast measure (LBP/C) was also calculated. In the LBP method, the eight neighbor pixels for each pixel in the ROI were examined and an 8-bit LBP-value and LBP/C were calculated (Figure 3). Weight positions in the LBP weight matrix were set to be perpendicular to bone fibers to get better enhancement of the fibers.

The Laplacian-based image was constructed as previously described[25]. However, since the ROIs were not oriented totally along the bone fibers, in addition to vertical direction, the Laplacian was calculated also in horizontal direction and summed into one matrix. Subsequently, the unprocessed ROI was multiplied with square root of the Laplacian matrix to enhance the bone and grayscale values were expanded to full dynamic range to obtain the final Laplacian-based image.

Entropy of the LBP-based ($E_{LBP}$) and Laplacian-based ($E_{Lap}$) image was calculated as follows:

$$E = -\Sigma_i P_i log_2 P_i, \quad (1)$$

where $P_i$ contains the normalized count of the grayscale value *i* occurring in the image. Entropy describes the distribution of the local patterns in the LBP method and the distribution of the grayscale values in the Laplacian method. If $E_{LBP} = 0$, there is only single pattern occurring in the original image, whereas $E_{Lap} = 0$ means that all pixel values in the Laplacian-based image are the same.

A texture measure called homogeneity index (HI) was calculated from LBP-based ($HI_{LBP}$) and Laplacian-based ($HI_{Lap}$) images. HI was derived from the gray-level co-occurrence matrix (GLCM)[30] that was calculated to the horizontal (0°) and vertical (90°) directions using one pixel distance. Mean HI of these directions was calculated to capture differences in the adjacent pixels in the image in these directions, since the bone fibers were not oriented along the image[31]. If all adjacent pixel values in an image are the same, HI is one.

### 2.6. Statistical analysis

Statistical analyses were performed using SPSS 19 software (SPSS Inc., Chicago, USA). Differences between KL-groups were evaluated using the linear mixed model. This method was chosen to adjust the correlation between the knees. In the model, KL group and knee (left or right) were set as fixed variables and patient was set as random variable. Restricted maximum Likelihood estimation was used in the model. Furthermore, estimated means for the different KL groups were obtained from the fitted model, and Fisher's least significant difference (LSD) test was performed to find out which KL groups differed statistically significantly from each other. In addition, Bonferroni post-hoc test was also performed to control multiple comparisons between KL groups. However, *p*-values obtained from the linear mixed models for different parameters were not adjusted for multiple comparisons[32]. Level of statistical significance was set to $p<0.05$.

To evaluate intra-rater reproducibility, one investigator (JH) performed the analyses for a sub-population of 70 knees (38 controls, 32 OA) three times with 2 weeks intervals. To evaluate inter-rater reproducibility, three investigators (JH, JT, VI) performed the analyses once for the same sub-population. The reproducibility of the bone parameters was evaluated using root-mean-square average coefficient of variation ($CV_{RMS}$)[33] according the following equation:

$$CV_{RMS} = \sqrt{\frac{\sum_{j=1}^{n}(CV_j)^2}{n}}, \quad (2)$$

where $CV_j$ is the individual coefficient of variation for the subject *j* and *n* is the number of the knees. The 95% confidence intervals for the $CV_{RMS}$ values were computed using the chi-square distribution[33].

## 3. Results

Altogether 110 knees were classified as KL0, 28 as KL1, 27 as KL2, 31 as KL3, and 7 as KL4. There were no statistically significant differences in age between different KL groups ($p = 0.179$).

### 3.1. Reproducibility

Both the intra-rater and inter-rater reproducibilities of the texture parameters were higher than the bone density-related parameters (Table 1). Particularly, $HI_{LBP}$, $E_{LBP}$, and $E_{Lap}$ were highly reproducible (intra- and inter-rater $CV_{RMS}$ values < 1.59%).

### 3.2. JSW

Medial JSW and mJSW were significantly ($p<0.05$) higher in the control group (KL0) than in the KL2-4 groups (Table 2).

### 3.3. Bone density-related parameters

Bone density-related grayscale values (GV, GV', and $GV_{norm}$) were significantly higher in the KL2-4 groups than in the KL0 group in the medial subchondral bone plate (Figure 4, Table 2).

In the medial subchondral trabecular bone, GV, GV', and $GV_{norm}$ were significantly higher in the KL2-4 groups than in the KL0 group (Figure 4, Table 3).

In the medial femur, GV was significantly higher in the KL2-4 groups and GV' in the KL3-4 groups than in the KL0 group (Table 4).

### 3.4. Bone structure-related parameters

In the medial subchondral bone plate, texture parameters $E_{Lap}$ (Figure 4), $HI_{LBP}$, and LBP/C were significantly higher and $E_{LBP}$ (Figure 4) lower in the KL2-4 groups than in the KL0 group (Table 2).

In the tibial trabecular bone, $E_{LBP}$ was significantly higher (Figure 4) and $HI_{LBP}$ lower in the KL1-4 groups than in the KL0 group in both medial and lateral sides (Table 3).

In femur, when compared to KL0, $E_{LBP}$ was significantly higher in the KL1-4 groups in medial side and in the KL2-4 groups in lateral side, whereas $E_{Lap}$ was significantly lower in the KL2-4 groups in the medial femur (Table 4).




Europe PMC Funders Author Manuscripts

Europe PMC Funders Author Manuscripts

## 4. Discussion

In the present study, we hypothesized that since both bone density and structure are altered during OA[1], these variations can be quantified using advanced image analysis of plain radiographs. This hypothesis was confirmed, yet the levels of variations depended on the site of analysis. Both density-related parameters and structure-related parameters showed significant differences between KL groups, particularly in the medial side.

The better intra-rater and inter-rater reproducibilities of the texture parameters suggest that they are more robust and user-independent choices for quantitative analysis of bone from plain radiographs than direct evaluation of grayscale values. It is also notable that the reproducibilities of these texture parameters are better than reproducibility of semi-quantitative KL grading[7-9]. In general, the intra-rater and inter-rater reproducibilities of the bone density-related parameters, particularly GV', were poor. Besides the bone ROI, user selects also a soft tissue ROI when calculating that parameter which produces an additional error source to GV'.

In all medial side ROIs, bone density increased along the severity of OA (KL grades). Consistently, in a previous study densities in medial subchondral bone in tibia and in femur were significantly higher in the OA than in the control group[12]. In that study, the bone density was estimated by comparing the intensity values in bone and in aluminum step wedge. Our results indicate that increased bone density (sclerosis) can be directly quantified if the X-ray imaging conditions are constant between patients. However, if the imaging conditions (geometry, imaging parameters, pre-processing, etc.) vary, plain mean values are not suitable for direct estimation of sclerosis. Furthermore, it is known that knee alignment is altered during OA[34], and that there is also variation in the intensity in the X-ray beam (*i.e.*, heel effect) that may also affect the measured grayscale values. The heel effect may also be a problem particularly if the cathode–anode axis orientation changes or if there is a great difference in the location of the knee on the film between study subjects.

We showed in this study that bone structure immediately under the cartilage–bone interface in the medial side is different between groups with different radiological stage of OA. This is promising finding as previously same kinds of results were obtained when OA patients were divided into the subgroups based on their mJSW[17, 35]. In the subchondral trabecular bone in tibia, structural changes detected mainly by the LBP-based parameters are in line with previous studies with fractal-based algorithms from radiographs[21, 23]. However, these studies had lower sample size and all OA patients were grouped in the same group and thus, OA subgroups were not compared. When investigating progression of OA, FSA and SDM methods from the medial subchondral trabecular bone in tibia predicted loss of medial joint space[14, 15, 22]. In addition to tibial bone changes, we found significant structural differences also from femur even between control and early OA groups. Based on our results, analysis of structural changes from femur during OA should also be considered in the future studies. However, the anatomical shape of the femur may complicate at least the evaluation of the bone density-related parameters, and may be one reason for the low number of studies concentrating quantitative analysis of this region.

In general, structural analysis of bone may not be as depended of imaging conditions as plain grayscale values. In the current study, we applied Laplacian- and LBP-based methods to study the bone structure. In the LBP method, the surrounding pixels affect the final LBP value but the magnitude of grayscale value differences is ignored. Therefore, complementary contrast measure, *i.e.* LBP/C, was also calculated. In contrary to LBP, grayscale values of the original image affect directly the Laplacian-based image. We observed that $E_{Lap}$ decreased whereas $E_{LBP}$ increased along the severity of OA. This inverse relation between these parameters is related to fundamental mathematical differences between LBP and Laplacian methods. According to conventional definition of entropy, lower entropy value indicates less randomness of the pixel values inside the ROI. When $E_{Lap}$ measures the randomness of the pixel values related to original image, $E_{LBP}$ actually measures the randomness of the different patterns in the original image. Trabecular bone volume is increased in OA mainly through reduced separation between trabeculae and an increase in trabecular number[2]. Therefore, the decrease in $E_{Lap}$ may be related to increased bone volume and consequently, less variation in the pixel values within the ROI is detected. Suitability of $E_{Lap}$ to X-ray image analysis was demonstrated also in the previous study of our group, in which $E_{Lap}$ discriminated hip fracture cases from controls[25]. The increase in $E_{LBP}$ suggests that variation in LBP in the image is greater in advanced OA, probably due to bone sclerosis. The decrease in $HI_{LBP}$ supports the conclusion since it indicated that adjacent patterns differed more from each other in advanced OA. Laplacian-based parameters were less sensitive to changes in trabecular bone which might indicate the better sensitivity of LBP-based method for bone structural changes. However, since this is apparently the first time to apply these LBP-based methods to the analyses of bone in the knee, further studies are needed to fully understand the relation between LBP-based parameters and actual structure of bone.

In addition to the methods used in this study, many different kinds of texture analysis methods for analyzing bone from plain radiographs have been introduced. Fractal-based analysis measuring the roughness of the image is one of the most popular methods. Fractal dimension of bone can be measured using several different methods[36], but in OA studies, FSA seems to be the most popular one[17-20, 22, 35, 37]. Compared to the methods used in this study, one major difference in the FSA method is that fractal dimensions are calculated in horizontal and vertical direction at different image scales, whereas entropies calculated from LBP- and Laplacian-based images are rotationally invariant. Furthermore, the mean values of vertical and horizontal directions of LBP- and Laplacian-based HIs were used in this study. Recently, methods that calculate fractals in all possible directions have also been presented[21, 23]. In the study of Woloszynski et al. (2010), rotation invariant texture classification accuracy of SDM and LBP methods were compared using a well-defined texture image dataset[38]. Although the dataset did not contain images from bone, circular LBP performed slightly better than SDM with smaller images (16×16 and 30×30 pixels) and with larger image sizes these two methods were comparable. In the current study, we, however, decided to use a squared LBP operator to avoid interpolation of pixel values which is required if the neighborhood is chosen to be circular. Detailed comparison between LBP, Laplacian, FSA, and other texture methods is a challenging topic that will require further

Europe PMC Funders Author Manuscripts

evaluation in the future to establish an optimal procedure including multiple parameters for bone texture analysis[39].

Although we observed more significant changes in the medial side, consistent with our results from the lateral side, loss of bone and bone structure has been also detected in earlier studies[14, 16, 17, 21, 23, 40]. The knees with medial compartment OA have usually varus malalignment[34] and therefore the loss of bone and bone structure in the lateral side could be a result of the associated subluxation and reduction in loading of this compartment[16, 17].

This study contains limitations that need to be addressed. First, quantitative results were compared to semi-quantitative KL grading, which was also conducted from the same image. Visual evaluation of subchondral sclerosis is also included in the KL grading, thus making quantitative image analysis results at least slightly dependent on the KL grade. Furthermore, KL grading is only based on a subjective evaluation of the changes in the joint. Therefore, in the future these advanced image analysis methods should be compared with independent methods that can give true information about the bone volumetric structure (*e.g.*, computed tomography). Second, we were unable to assess how well our parameters predicted the progression of OA since our study was cross-sectional. Third, the heel effect may have affected the measured grayscale values. However, in theory, the texture parameters should be less affected by the heel effect. For example, LBP parameters provide highly localized measures of bone texture and are insensitive to monotonic grayscale variations. Fourth, it is unclear how much the reproducibility of each parameter is affected by a pixel shift error when manually placing the ROIs. Therefore, presumably a more robust method to place the ROIs (*e.g.*, automated placement) would improve the reproducibility. These limitations should be carefully addressed in future studies.

In conclusion, our results indicate that changes in bone texture parameters in knee OA can be quantitatively evaluated from plain radiographs using the presented methods. The most significant changes were seen in the medial subchondral bone plate and trabecular bone in proximal tibia and in medial femur. Structural analysis of bone was more reproducible than direct evaluation of grayscale values, and it is therefore better suited for quantitative analysis when imaging conditions are variable.

## Acknowledgements

The authors thank Mr Risto Bloigu, MSc, for statistical consultancy.

**Role of the funding source**

The research leading to these results has received funding from the Finnish Cultural Foundation, University of Oulu (strategic funding), Academy of Finland (grant 268378), Kuopio University Hospital (EVO grant), and European Research Council under the European Union's Seventh Framework Programme (FP/2007-2013) / ERC Grant Agreement no. 336267. The funding sources had no role in the study design, data collection or analysis, interpretation of data, writing of the manuscript, or in the decision to submit the manuscript for publication.

## References

1. Buckwalter JA, Mankin HJ. Articular cartilage: degeneration and osteoarthritis, repair, regeneration, and transplantation. Instr.Course Lect. 1998; 47:487–504. [PubMed: 9571450]

2. Burr DB. Anatomy and physiology of the mineralized tissues: role in the pathogenesis of osteoarthrosis. Osteoarthritis Cartilage. 2004; 12:S20–30. [PubMed: 14698637]
3. Goldring MB, Goldring SR. Articular cartilage and subchondral bone in the pathogenesis of osteoarthritis. Ann.N.Y.Acad.Sci. 2010; 1192:230–7. [PubMed: 20392241]
4. Madry H, van Dijk CN, Mueller-Gerbl M. The basic science of the subchondral bone. Knee Surg.Sports Traumatol.Arthrosc. 2010; 18:419–33. [PubMed: 20119671]
5. Buckwalter JA, Martin JA. Osteoarthritis. Adv.Drug Deliv.Rev. 2006; 58:150–67. [PubMed: 16530881]
6. Kellgren JH, Lawrence JS. Radiological assessment of osteo-arthrosis. Ann.Rheum.Dis. 1957; 16:494–502. [PubMed: 13498604]
7. Spector TD, Dacre JE, Harris PA, Huskisson EC. Radiological progression of osteoarthritis: an 11 year follow up study of the knee. Ann.Rheum.Dis. 1992; 51:1107–10. [PubMed: 1444622]
8. Spector TD, Hart DJ, Byrne J, Harris PA, Dacre JE, Doyle DV. Definition of osteoarthritis of the knee for epidemiological studies. Ann.Rheum.Dis. 1993; 52:790–4. [PubMed: 8250610]
9. Gunther KP, Sun Y. Reliability of radiographic assessment in hip and knee osteoarthritis. Osteoarthritis Cartilage. 1999; 7:239–46. [PubMed: 10222223]
10. Buckland-Wright C. Radiographic assessment of osteoarthritis: comparison between existing methodologies. Osteoarthritis Cartilage. 1999; 7:430–3. [PubMed: 10419790]
11. Reichmann WM, Maillefert JF, Hunter DJ, Katz JN, Conaghan PG, Losina E. Responsiveness to change and reliability of measurement of radiographic joint space width in osteoarthritis of the knee: a systematic review. Osteoarthritis Cartilage. 2011; 19:550–6. [PubMed: 21396469]
12. Marijnissen AC, Vincken KL, Vos PA, Saris DB, Viergever MA, Bijlsma JW, et al. Knee Images Digital Analysis (KIDA): a novel method to quantify individual radiographic features of knee osteoarthritis in detail. Osteoarthritis Cartilage. 2008; 16:234–43. [PubMed: 17693099]
13. Kinds MB, Bartels LW, Marijnissen AC, Vincken KL, Viergever MA, Lafeber FP, et al. Feasibility of bone density evaluation using plain digital radiography. Osteoarthritis Cartilage. 2011; 19:1343–8. [PubMed: 21884807]
14. Woloszynski T, Podsiadlo P, Stachowiak GW, Kurzynski M, Lohmander LS, Englund M. Prediction of progression of radiographic knee osteoarthritis using tibial trabecular bone texture. Arthritis Rheum. 2012; 64:688–95. [PubMed: 21989629]
15. Kraus VB, Feng S, Wang S, White S, Ainslie M, Le Graverand M-H, et al. Subchondral bone trabecular integrity predicts and changes concurrently with radiographic and magnetic resonance imaging-determined knee osteoarthritis progression. Arthritis Rheum. 2013; 65:1812–21. [PubMed: 23576116]
16. Buckland-Wright C. Subchondral bone changes in hand and knee osteoarthritis detected by radiography. Osteoarthritis Cartilage. 2004; 12:S10–9. [PubMed: 14698636]
17. Messent EA, Ward RJ, Tonkin CJ, Buckland-Wright C. Cancellous bone differences between knees with early, definite and advanced joint space loss; a comparative quantitative macroradiographic study. Osteoarthritis Cartilage. 2005; 13:39–47. [PubMed: 15639636]
18. Messent EA, Ward RJ, Tonkin CJ, Buckland-Wright C. Tibial cancellous bone changes in patients with knee osteoarthritis. A short-term longitudinal study using Fractal Signature Analysis. Osteoarthritis Cartilage. 2005; 13:463–70. [PubMed: 15922180]
19. Messent EA, Ward RJ, Tonkin CJ, Buckland-Wright C. Osteophytes, juxta-articular radiolucencies and cancellous bone changes in the proximal tibia of patients with knee osteoarthritis. Osteoarthritis Cartilage. 2007; 15:179–86. [PubMed: 16905342]
20. Messent EA, Ward RJ, Tonkin CJ, Buckland-Wright C. Differences in trabecular structure between knees with and without osteoarthritis quantified by macro and standard radiography, respectively. Osteoarthritis Cartilage. 2006; 14:1302–5. [PubMed: 16990028]
21. Podsiadlo P, Dahl L, Englund M, Lohmander LS, Stachowiak GW. Differences in trabecular bone texture between knees with and without radiographic osteoarthritis detected by fractal methods. Osteoarthritis Cartilage. 2008; 16:323–9. [PubMed: 17825585]
22. Kraus VB, Feng S, Wang S, White S, Ainslie M, Brett A, et al. Trabecular morphometry by fractal signature analysis is a novel marker of osteoarthritis progression. Arthritis Rheum. 2009; 60:3711–22. [PubMed: 19950282]

23. Wolski M, Podsiadlo P, Stachowiak GW, Lohmander LS, Englund M. Differences in trabecular bone texture between knees with and without radiographic osteoarthritis detected by directional fractal signature method. Osteoarthritis Cartilage. 2010; 18:684–90. [PubMed: 20175970]
24. Pulkkinen P, Partanen J, Jalovaara P, Nieminen M, Jämsä T. Combination of radiograph-based trabecular and geometrical parameters can discriminate cervical hip fractures from controls in individuals with BMD in non-osteoporotic range. Bone. 2011; 49:290–4. [PubMed: 21550431]
25. Thevenot J, Hirvasniemi J, Pulkkinen P, Määttä M, Korpelainen R, Saarakkala S, et al. Assessment of risk of femoral neck fracture with radiographic texture parameters: a retrospective study. Radiology. 2014 doi: http://dx.doi.org/10.1148/radiol.14131390.
26. Ojala T, Pietikäinen M, Harwood D. A comparative study of texture measures with classification based on feature distributions. Pattern Recogn. 1996; 29:51–9.
27. Houam L, Hafiane A, Boukrouche A, Lespessailles E, Jennane R. One dimensional local binary pattern for bone texture characterization. Pattern Anal.Appl. 2012:1–15.
28. Liikavainio T, Bragge T, Hakkarainen M, Karjalainen PA, Arokoski JP. Gait and muscle activation changes in men with knee osteoarthritis. Knee. 2010; 17:69–76. [PubMed: 19556137]
29. Liikavainio T, Lyytinen T, Tyrvainen E, Sipila S, Arokoski JP. Physical function and properties of quadriceps femoris muscle in men with knee osteoarthritis. Arch.Phys.Med.Rehabil. 2008; 89:2185–94. [PubMed: 18996249]
30. Haralick RM, Shanmugam K, Dinstein I. Textural features for image classification. IEEE Trans.Syst.Man Cybern. 1973; smc 3:610–21.
31. Thevenot J, Hirvasniemi J, Finnilä M, Pulkkinen P, Kuhn V, Link T, et al. Trabecular homogeneity index derived from plain radiograph to evaluate bone quality. J Bone Miner Res. 2013; 28:2584–91. [PubMed: 23677814]
32. Rothman KJ. No adjustments are needed for multiple comparisons. Epidemiology. 1990; 1:43–6. [PubMed: 2081237]
33. Gluer CC, Blake G, Lu Y, Blunt BA, Jergas M, Genant HK. Accurate assessment of precision errors: how to measure the reproducibility of bone densitometry techniques. Osteoporos.Int. 1995; 5:262–70. [PubMed: 7492865]
34. Sharma L, Song J, Felson DT, Cahue S, Shamiyeh E, Dunlop DD. The role of knee alignment in disease progression and functional decline in knee osteoarthritis. JAMA. 2001; 286:188–95. [PubMed: 11448282]
35. Buckland-Wright JC, Lynch JA, Macfarlane DG. Fractal signature analysis measures cancellous bone organisation in macroradiographs of patients with knee osteoarthritis. Ann.Rheum.Dis. 1996; 55:749–55. [PubMed: 8984941]
36. Geraets WG, van der Stelt PF. Fractal properties of bone. Dentomaxillofac.Radiol. 2000; 29:144–53. [PubMed: 10849540]
37. Lynch JA, Hawkes DJ, Buckland-Wright JC. A robust and accurate method for calculating the fractal signature of texture in macroradiographs of osteoarthritic knees. Med.Inform.(Lond). 1991; 16:241–51. [PubMed: 1921566]
38. Woloszynski T, Podsiadlo P, Stachowiak GW, Kurzynski M. A signature dissimilarity measure for trabecular bone texture in knee radiographs. Med.Phys. 2010; 37:2030–42. [PubMed: 20527536]
39. Huber MB, Carballido-Gamio J, Fritscher K, Schubert R, Haenni M, Hengg C, et al. Development and testing of texture discriminators for the analysis of trabecular bone in proximal femur radiographs. Med.Phys. 2009; 36:5089–98. [PubMed: 19994519]
40. Lindsey CT, Narasimhan A, Adolfo JM, Jin H, Steinbach LS, Link T, et al. Magnetic resonance evaluation of the interrelationship between articular cartilage and trabecular bone of the osteoarthritic knee. Osteoarthritis Cartilage. 2004; 12:86–96. [PubMed: 14723868]

Europe PMC Funders Author Manuscripts

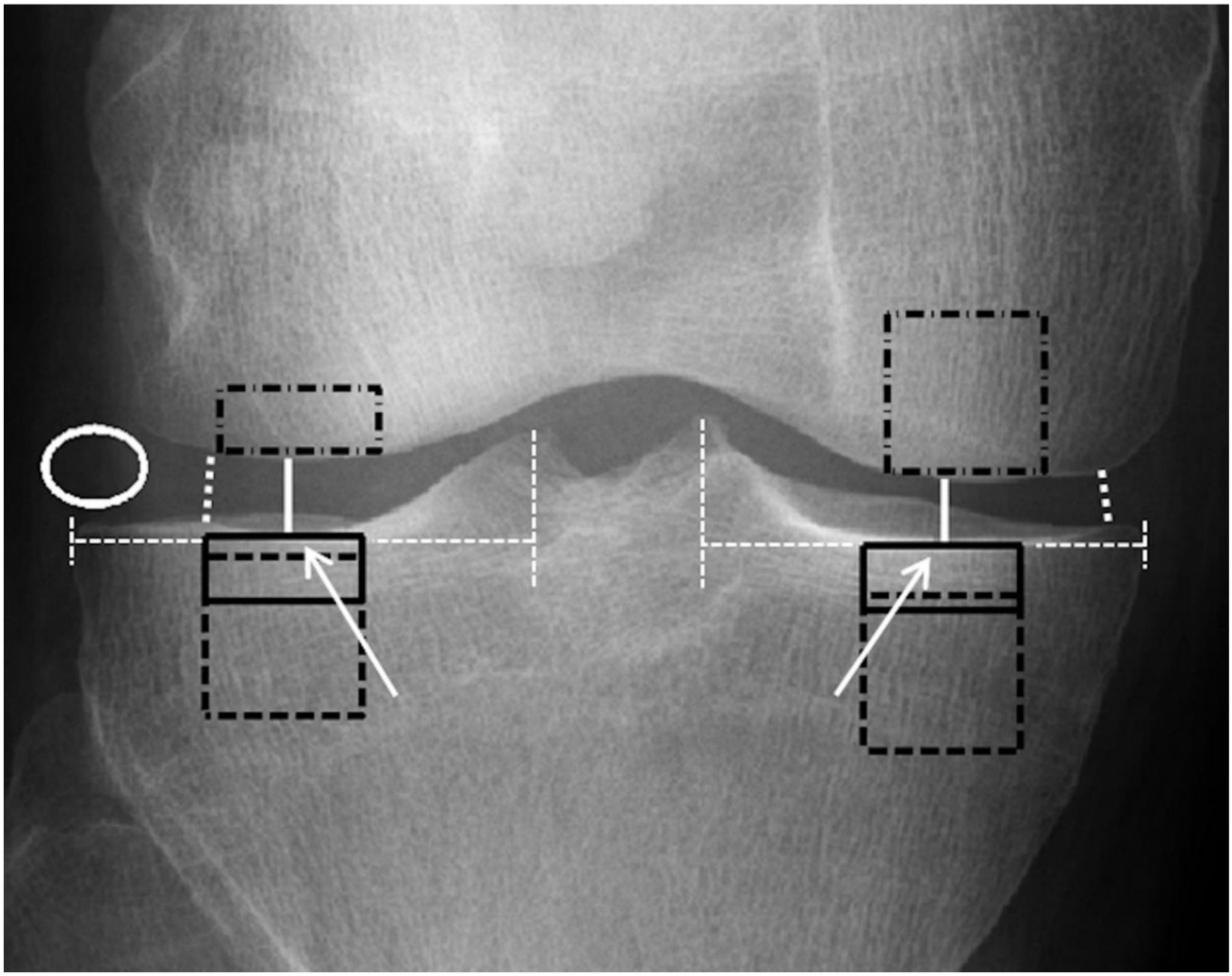

**Figure 1.**

A schematic figure describing manual placement of ROIs. Subchondral bone plate ROIs were placed immediately under the cartilage–bone interface in the middle part of medial and lateral condyles of tibia (ROIs shown with black-colored rectangles with continuous line). The center points (white arrows) were checked visually and they were about a half of the horizontal distance between the outer border of tibia and a vertical line drawn from the medial or lateral tibial spine (white dashed lines). Subchondral trabecular bone ROIs (black squares with dashed line) were placed immediately below the subchondral bone plate of tibia and were aligned horizontally with the subchondral bone plate ROIs. When placing femur ROIs (black rectangles with dash-dotted line), horizontal alignment of subchondral bone plate ROIs, plateau in the middle part of femoral condyles, and patella were considered. JSWs, shown with white continuous line, and minimum JSWs (white dotted line) were measured manually from the middle part of the condyles and from the narrowest point of the joint, respectively. Soft tissue ROI (white ellipse) was placed in the lateral side of the joint. For more details, see the Methods section.

Europe PMC Funders Author Manuscripts

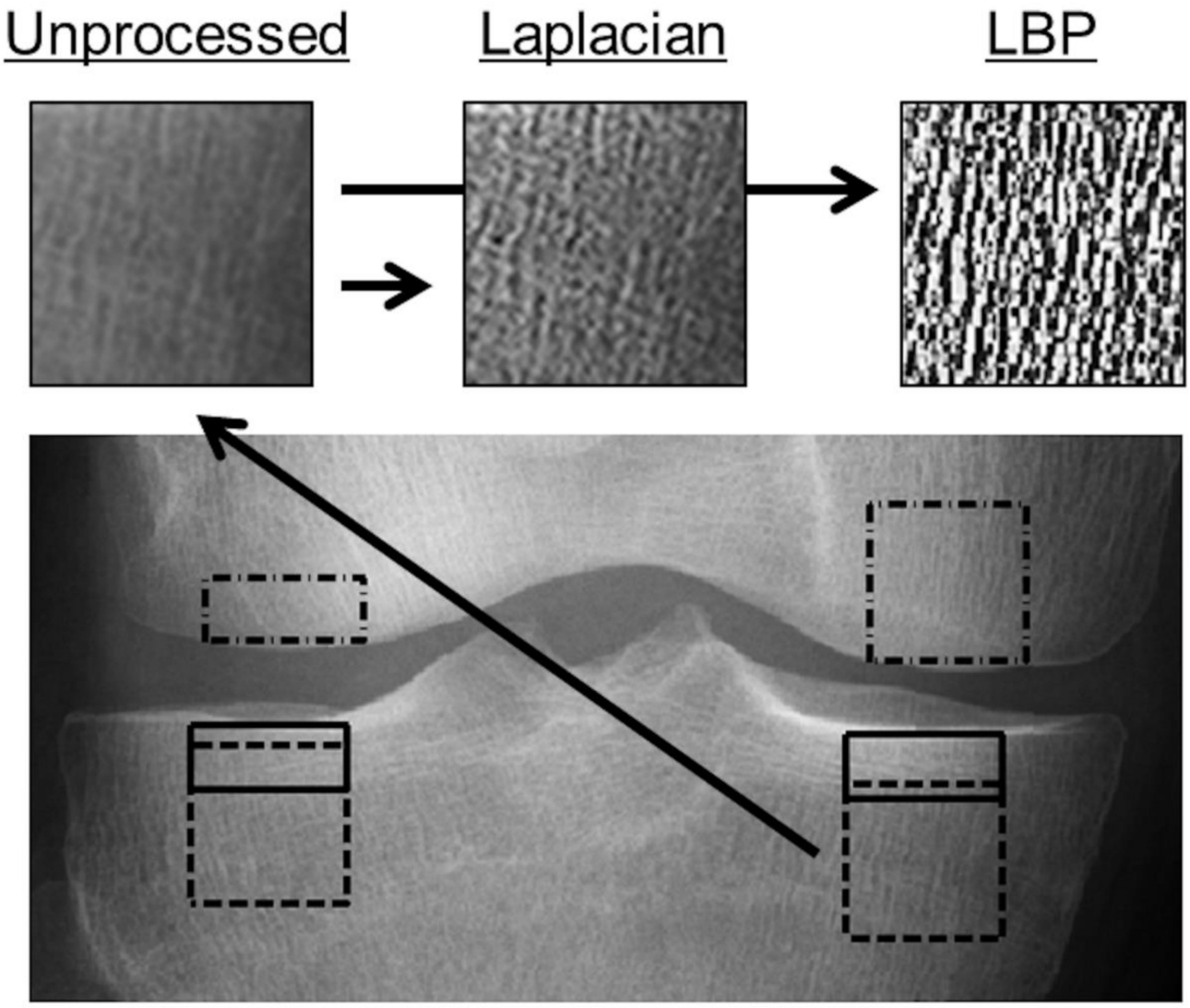


**Figure 2.**
An illustrative presentation of unprocessed ROI, Laplacian-based ROI, and LBP-based ROI from medial subchondral trabecular bone in proximal tibia.

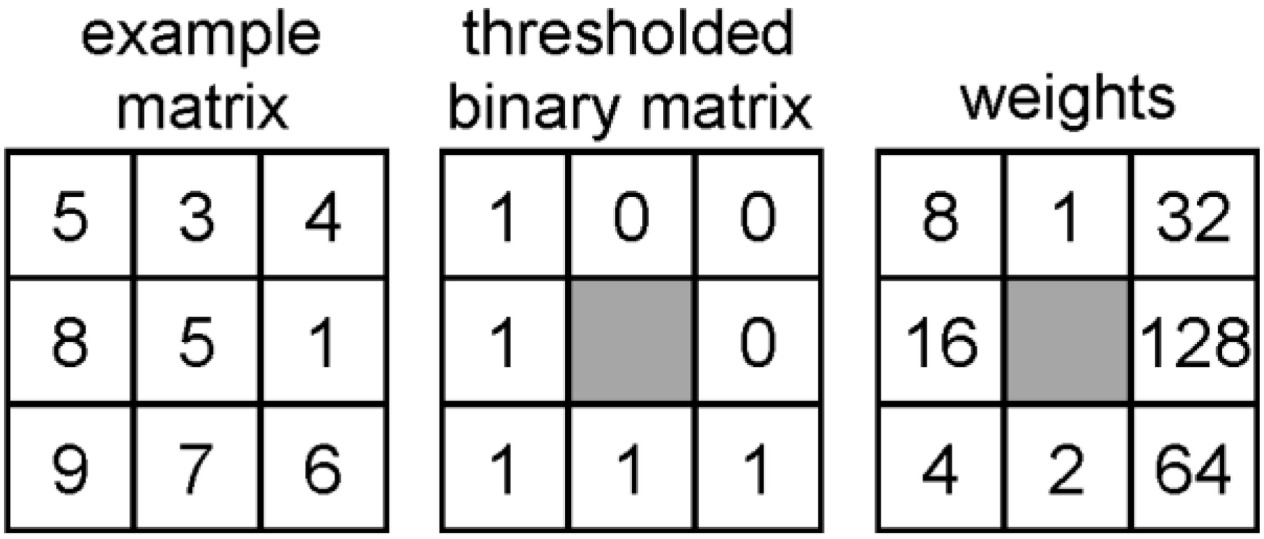


**Figure 3.**

LBP is built by thresholding neighbor pixels by the grayscale value of the center pixel and multiplying the binary matrix with the weight matrix. Weights were set to be perpendicular to bone fibers to get better enhancement of the fibers. In this example LBP = 1*8+0*1+0*32+0*128+1*64+1*2+1*4+1*16 = 94. LBP based contrast value (LBP/C) is calculated as follows = (5+6+7+9+8)/5 − (3+4+1)/3 = 4.3.



Europe PMC Funders Author Manuscripts

Europe PMC Funders Author Manuscripts

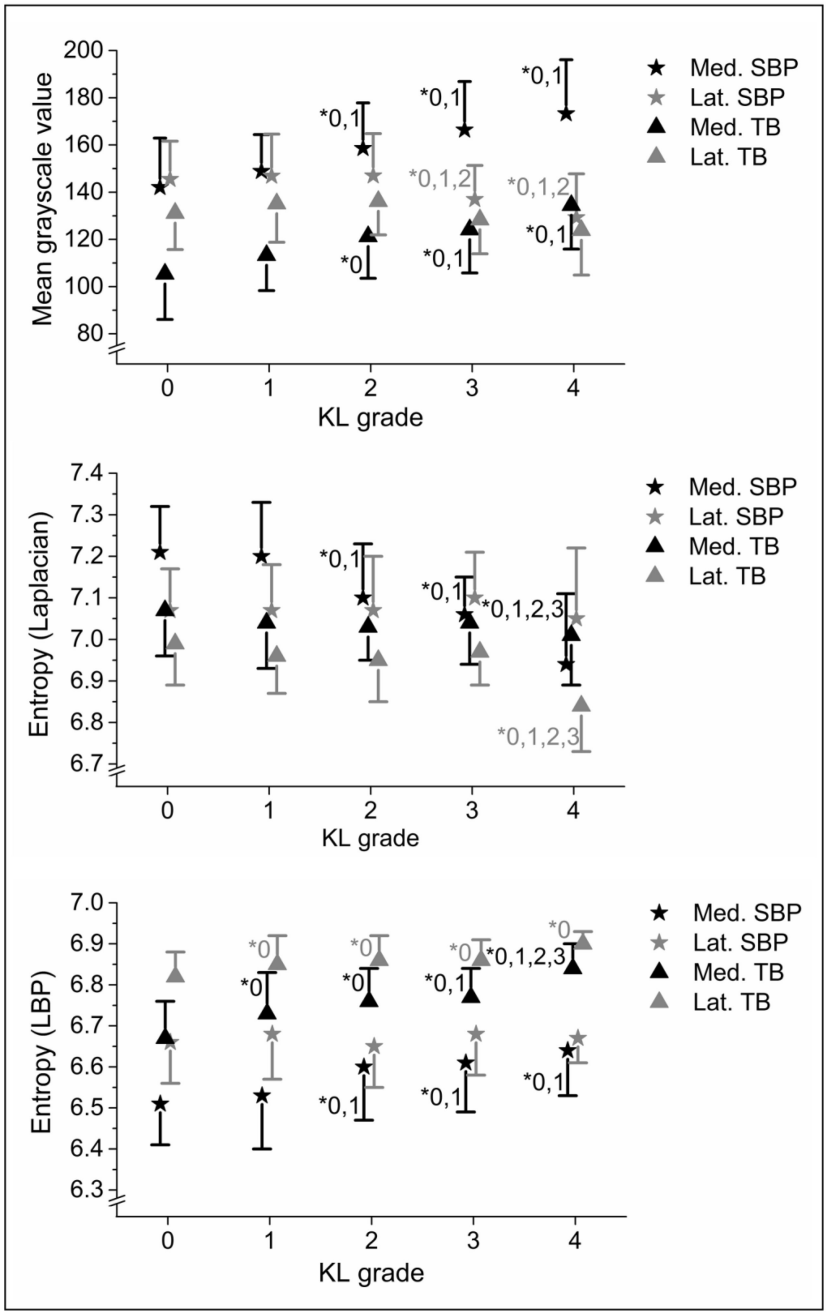


**Figure 4.**

Statistically significant differences between KL groups in medial and lateral tibial subchondral bone plate (SBP) and trabecular bone (TB) using GV and entropy from both Laplacian-based ($E_{Lap}$) and LBP images ($E_{LBP}$). * = Studied KL group differs significantly from the indicated KL group (LSD post-hoc test).

Europe PMC Funders Author Manuscripts

## Table 1

The intra-rater and inter-rater reproducibilities (root-mean-square average coefficient of variation values [%]) of the variables.

| | Subchondral bone plate | | Trabecular bone | | Femur | |
|---|---|---|---|---|---|---|
| **Parameter** | **Medial** | **Lateral** | **Medial** | **Lateral** | **Medial** | **Lateral** |
| **Intra-rater reproducibility** | | | | | | |
| GV | 2.78 (2.23 – 3.56) | 2.79 (2.24 – 3.58) | 2.62 (2.10 – 3.36) | 1.45 (1.16 – 1.86) | 3.05 (2.45 – 3.92) | 5.06 (4.05 – 6.49) |
| GV’ | 7.13 (5.71 – 9.15) | 6.68 (5.36 – 8.57) | 13.99 (11.21 – 17.94) | 8.91 (7.14 – 11.42) | 9.53 (7.64 – 12.23) | 8.36 (6.70 – 10.73) |
| $GV_{norm}$ | 2.77 (2.22 – 3.55) | 2.69 (2.16 – 3.46) | 2.70 (2.17 – 3.47) | 1.56 (1.25 – 2.00) | - | - |
| LBP/C | 3.33 (2.67 – 4.27) | 4.71 (3.77 – 6.04) | 1.45 (1.16 – 1.85) | 1.93 (1.54 – 2.47) | 1.37 (1.10 – 1.76) | 2.68 (2.15 – 3.44) |
| $HI_{Lap}$ | 2.17 (1.74 – 2.79) | 2.46 (1.97 – 3.16) | 1.64 (1.31 – 2.10) | 1.98 (1.58 – 2.54) | 1.32 (1.06 – 1.69) | 1.88 (1.51 – 2.41) |
| $HI_{LBP}$ | 0.85 (0.68 – 1.09) | 0.93 (0.75 – 1.19) | 0.51 (0.41 – 0.65) | 0.75 (0.60 – 0.96) | 0.70 (0.56 – 0.90) | 1.02 (0.82 – 1.31) |
| $E_{Lap}$ | 1.46 (1.17 – 1.87) | 1.59 (1.27 – 2.04) | 0.74 (0.59 – 0.95) | 1.01 (0.81 – 1.29) | 0.70 (0.56 – 0.89) | 0.94 (0.75 – 1.20) |
| $E_{LBP}$ | 0.42 (0.34 – 0.54) | 0.56 (0.44 – 0.71) | 0.23 (0.18 – 0.29) | 0.26 (0.21 – 0.33) | 0.29 (0.23 – 0.37) | 0.35 (0.28 – 0.44) |
| **Inter-rater reproducibility** | | | | | | |
| GV | 4.37 (3.50 – 5.60) | 3.10 (2.49 – 3.98) | 4.33 (3.47- 5.55) | 2.51 (2.01 – 3.21) | 4.75 (3.81 – 6.09) | 6.11 (4.90 – 7.83) |
| GV’ | 11.85 (9.50 – 15.21) | 9.45 (7.58 – 12.13) | 22.19 (17.79 – 28.47) | 12.56 (10.07 – 16.11) | 16.21 (13.00 – 20.80) | 12.19 (9.77 – 15.64) |
| $GV_{norm}$ | 4.54 (3.64 – 5.82) | 4.00 (3.21 – 5.13) | 4.13 (3.31 – 5.30) | 2.47 (1.98 – 3.17) | - | - |
| LBP/C | 3.19 (2.55 – 4.09) | 3.27 (2.62 – 4.19) | 2.49 (2.00 – 3.20) | 1.93 (1.55 -2.48) | 2.21 (1.77 – 2.83) | 3.20 (2.56 – 4.10) |
| $HI_{Lap}$ | 1.74 (1.39 – 2.23) | 1.90 (1.53 – 2.44) | 2.48 (1.99 – 3.19) | 2.05 (1.64 – 2.63) | 1.51 (1.21 – 1.94) | 2.04 (1.63 – 2.62) |
| $HI_{LBP}$ | 0.95 (0.76 – 1.22) | 1.04 (0.84 – 1.34) | 0.67 (0.53 – 0.85) | 0.90 (0.72 – 1.15) | 1.06 (0.85 – 1.35) | 1.25 (1.00 – 1.60) |
| $E_{Lap}$ | 0.88 (0.70 – 1.13) | 0.89 (0.71 – 1.14) | 1.00 (0.80 – 1.28) | 1.04 (0.84 – 1.34) | 0.99 (0.79 – 1.27) | 1.07 (0.86 – 1.37) |
| $E_{LBP}$ | 0.57 (0.46 – 0.73) | 0.52 (0.42 – 0.67) | 0.31 (0.25 – 0.40) | 0.29 (0.23 – 0.37) | 0.41 (0.33 – 0.53) | 0.39 (0.31 – 0.50) |

Values in parentheses are the 95% confidence interval. GV = mean grayscale value, GV’ = soft tissue subtracted from GV, $GV_{norm}$ = GV divided by the depth of the tibia, LBP/C = local binary patterns based contrast measure, $HI_{Lap}$ = homogeneity index from Laplacian-based image, $HI_{LBP}$ = homogeneity index from LBP-based image, $E_{Lap}$ = entropy from Laplacian-based image, and $E_{LBP}$ = entropy from LBP-based image.

## Table 2

Mean (SD) values of medial and lateral JSW, minimum JSWs (mJSW), and bone density-related and structure-related parameters in different KL grade groups from subchondral bone plate in tibia.

| Side | Parameter | KL0 (*n*=108-110) | KL1 (*n*=28) | KL2 (*n*=27) | KL3 (*n*=31) | KL4 (*n*=7) | *p*-value | Post-hoc* |
|---|---|---|---|---|---|---|---|---|
| Medial | JSW (mm) | 5.4 (0.9) | 5.0 (0.9) | 4.0 (1.1) | 3.0 (1.3) | 2.0 (1.6) | <0.001 | **0-2**, **0-3**, **0-4**, **1-2**, **1-3**, **1-4**, **2-3**, **2-4**, 3-4 |
| | mJSW (mm) | 4.2 (0.9) | 4.1 (1.0) | 2.9 (1.1) | 2.1 (1.1) | 1.7 (1.3) | <0.001 | **0-2**, **0-3**, **0-4**, **1-2**, **1-3**, **1-4**, **2-3**, 2-4 |
| | GV | 142 (21) | 149 (16) | 159 (19) | 166 (20) | 173 (23) | <0.001 | **0-2**, **0-3**, **0-4**, 1-2**, 1-3**, **1-4** |
| | GV’ | 97 (21) | 101 (23) | 107 (19) | 120 (20) | 126 (26) | <0.001 | 0-2, **0-3**, **0-4**, **1-3**, **1-4**, 2-3, 2-4 |
| | $GV_{norm}$ | 24.6 (3.8) | 25.2 (3.0) | 26.8 (3.4) | 27.8 (3.6) | 29.1 (4.5) | <0.001 | **0-2**, **0-3**, **0-4**, **1-3**, 1-4 |
| | LBP/C | 8.98 (1.10) | 8.91 (1.08) | 8.20 (1.42) | 7.69 (1.15) | 6.93 (0.61) | <0.001 | **0-2**, **0-3**, **0-4**, 1-2,**1-3**, **1-4**, 2-4 |
| | $HI_{Lap}$ | 0.70 (0.02) | 0.70 (0.02) | 0.71 (0.02) | 0.69 (0.02) | 0.70 (0.03) | 0.216 | - |
| | $HI_{LBP}$ | 0.46 (0.02) | 0.45 (0.02) | 0.45 (0.02) | 0.44 (0.02) | 0.43 (0.02) | <0.001 | **0-2**, **0-3**, **0-4**, **1-3**, **1-4** |
| | $E_{Lap}$ | 7.21 (0.11) | 7.20 (0.13) | 7.10 (0.13) | 7.06 (0.09) | 6.94 (0.17) | <0.001 | **0-2**, **0-3**, **0-4**, **1-2**, **1-3**, **1-4**, **2-4**, 3-4 |
| | $E_{LBP}$ | 6.51 (0.10) | 6.53 (0.13) | 6.60 (0.13) | 6.61 (0.12) | 6.64 (0.11) | <0.001 | **0-2**, **0-3**, **0-4**, 1-2**, 1-3,** 1-4 |
| Lateral | JSW (mm) | 6.2 (1.3) | 6.5 (0.8) | 6.2 (0.9) | 6.5 (1.4) | 8.0 (1.4) | 0.004 | **0-4**, **1-4**, **2-4**, **3-4** |
| | mJSW (mm) | 5.4 (1.2) | 5.6 (1.0) | 5.5 (1.0) | 5.6 (1.2) | 7.1 (1.2) | 0.009 | **0-4**, **1-4**, **2-4**, **3-4** |
| | GV | 145 (16) | 147 (18) | 147 (18) | 137 (14) | 129 (18) | 0.009 | 0-3, 0-4, 1-3, 1-4, 2-3, 2-4 |
| | GV’ | 101 (15) | 99 (14) | 96 (17) | 91 (15) | 81 (14) | 0.001 | **0-3**, **0-4**, 1-3, 1-4, 2-4 |
| | $GV_{norm}$ | 25.2 (2.9) | 24.8 (3.1) | 24.9 (3.2) | 22.9 (2.4) | 21.7 (3.5) | <0.001 | **0-3**, **0-4**, 1-3,1-4, 2-3, 2-4 |
| | LBP/C | 8.14 (1.11) | 8.18 (1.10) | 8.28 (1.06) | 8.34 (0.85) | 8.88 (1.28) | 0.437 | - |
| | $HI_{Lap}$ | 0.70 (0.02) | 0.70 (0.02) | 0.70 (0.02) | 0.70 (0.02) | 0.72 (0.03) | 0.064 | - |
| | $HI_{LBP}$ | 0.45 (0.02) | 0.44 (0.02) | 0.45 (0.02) | 0.44 (0.01) | 0.45 (0.01) | 0.337 | - |
| | $E_{Lap}$ | 7.07 (0.10) | 7.07 (0.11) | 7.07 (0.13) | 7.10 (0.11) | 7.05 (0.17) | 0.678 | - |
| | $E_{LBP}$ | 6.66 (0.10) | 6.68 (0.11) | 6.65 (0.10) | 6.68 (0.10) | 6.67 (0.06) | 0.713 | - |

* Differences between groups using Fisher’s LSD. Differences between groups using Bonferroni post-hoc test are bolded. GV = mean grayscale value, GV’ = soft tissue subtracted from GV, $GV_{norm}$ = GV divided by the depth of the tibia, LBP/C = local binary patterns based contrast measure, $HI_{Lap}$ = homogeneity index from Laplacian-based image, $HI_{LBP}$ = homogeneity index from LBP-based image, $E_{Lap}$ = entropy from Laplacian-based image, and $E_{LBP}$ = entropy from LBP-based image.

Europe PMC Funders Author Manuscripts

## Table 3

Mean (SD) values of density-related and structure-related parameters in different KL grade groups from medial and lateral subchondral trabecular bone in tibia.

| Side | Parameter | KL0 (*n*=104) | KL1 (*n*=28) | KL2 (*n*=27) | KL3 (*n*=31) | KL4 (*n*=7) | *p*-value | Post-hoc* |
|---|---|---|---|---|---|---|---|---|
| Medial | GV | 105 (19) | 113 (15) | 121 (18) | 124 (18) | 135 (19) | <0.001 | **0-2, 0-3, 0-4,** 1-3, **1-4** |
| | GV' | 60 (19) | 65 (17) | 70 (17) | 78 (16) | 87 (22) | <0.001 | 0-2, **0-3, 0-4**, **1-3**, **1-4**, 2-4 |
| | $GV_{norm}$ | 18.3 (3.4) | 19.1 (2.6) | 20.5 (3.0) | 20.7 (3.1) | 22.5 (3.4) | <0.001 | **0-2, 0-3, 0-4**, 1-3, 1-4 |
| | LBP/C | 8.03 (0.88) | 8.19 (0.52) | 8.12 (0.85) | 7.84 (0.79) | 7.14 (0.90) | 0.031 | 0-4, **1-4**, 2-4, 3-4 |
| | $HI_{Lap}$ | 0.72 (0.02) | 0.72 (0.03) | 0.72 (0.02) | 0.71 (0.02) | 0.70 (0.02) | 0.001 | **0-3**, **0-4**, 1-3, 1-4, 2-4 |
| | $HI_{LBP}$ | 0.48 (0.02) | 0.47 (0.02) | 0.47 (0.02) | 0.46 (0.02) | 0.44 (0.01) | <0.001 | 0-1, 0-2, **0-3, 0-4**, 1-3, **1-4**, **2-4**, 3-4 |
| | $E_{Lap}$ | 7.07 (0.11) | 7.04 (0.11) | 7.03 (0.08) | 7.04 (0.10) | 7.01 (0.12) | 0.113 | - |
| | $E_{LBP}$ | 6.67 (0.09) | 6.73 (0.10) | 6.76 (0.08) | 6.77 (0.07) | 6.84 (0.06) | <0.001 | **0-1, 0-2, 0-3, 0-4, 1-3, 1-4**, 2-4, 3-4 |
| Lateral | GV | 131 (16) | 135 (16) | 136 (14) | 128 (15) | 124 (19) | 0.148 | - |
| | GV' | 87 (13) | 87 (11) | 85 (12) | 82 (13) | 76 (17) | 0.169 | - |
| | $GV_{norm}$ | 22.8 (2.7) | 22.8 (2.8) | 23.0 (2.4) | 21.4 (2.4) | 20.8 (3.5) | 0.039 | **0-3**, 2-3, 2-4 |
| | LBP/C | 7.85 (0.77) | 7.88 (0.66) | 7.71 (0.80) | 7.78 (0.45) | 7.43 (1.10) | 0.531 | - |
| | $HI_{Lap}$ | 0.70 (0.02) | 0.70 (0.02) | 0.70 (0.02) | 0.70 (0.02) | 0.71 (0.02) | 0.144 | - |
| | $HI_{LBP}$ | 0.45 (0.01) | 0.45 (0.02) | 0.44 (0.02) | 0.44 (0.01) | 0.43 (0.01) | <0.001 | 0-1, **0-2, 0-3, 0-4** |
| | $E_{Lap}$ | 6.99 (0.10) | 6.96 (0.09) | 6.95 (0.10) | 6.97 (0.08) | 6.84 (0.11) | 0.002 | **0-4**, **1-4**, 2-4, **3-4** |
| | $E_{LBP}$ | 6.82 (0.06) | 6.85 (0.07) | 6.86 (0.06) | 6.86 (0.05) | 6.90 (0.03) | <0.001 | 0-1, **0-2, 0-3, 0-4** |

*Differences between groups using Fisher's LSD. Differences between groups using Bonferroni post-hoc test are bolded. GV = mean grayscale value, GV' = soft tissue subtracted from GV, $GV_{norm}$ = GV divided by the depth of the tibia, LBP/C = local binary patterns based contrast measure, $HI_{Lap}$ = homogeneity index from Laplacian-based image, $HI_{LBP}$ = homogeneity index from LBP-based image, $E_{Lap}$ = entropy from Laplacian-based image, and $E_{LBP}$ = entropy from LBP-based image.

## Table 4

Mean (SD) values of density-related and structure-related parameters in different KL grade groups from medial and lateral femur.

| Side | Parameter | KL0 (*n*=105-108) | KL1 (*n*=28) | KL2 (*n*=27) | KL3 (*n*=30-31) | KL4 (*n*=7) | *p*-value | Post-hoc* |
|---|---|---|---|---|---|---|---|---|
| Medial | GV | 130 (21) | 137 (18) | 139 (20) | 147 (19) | 159 (26) | <0.001 | 0-2**, 0-3, 0-4,** 1-3, 1-4, 2-4 |
| | GV' | 86 (24) | 89 (24) | 88 (21) | 101 (23) | 111 (29) | 0.002 | **0-3,** 0-4, 1-3, 1-4, 2-3, 2-4 |
| | LBP/C | 7.51 (0.77) | 7.65 (0.52) | 7.41 (0.93) | 7.44 (0.70) | 6.86 (0.50) | 0.159 | - |
| | $HI_{Lap}$ | 0.71 (0.02) | 0.70 (0.02) | 0.70 (0.01) | 0.69 (0.02) | 0.70 (0.01) | <0.001 | **0-1**, **0-2**, **0-3** |
| | $HI_{LBP}$ | 0.46 (0.02) | 0.45 (0.02) | 0.45 (0.02) | 0.45 (0.01) | 0.43 (0.01) | <0.001 | **0-3, 0-4,** 1-3, **1-4**, 2-4 |
| | $E_{Lap}$ | 7.13 (0.11) | 7.10 (0.10) | 7.02 (0.12) | 6.99 (0.11) | 6.92 (0.15) | <0.001 | **0-2, 0-3, 0-4, 1-2, 1-3, 1-4,** 2-4 |
| | $E_{LBP}$ | 6.72 (0.08) | 6.77 (0.09) | 6.80 (0.10) | 6.83 (0.06) | 6.90 (0.04) | <0.001 | 0-1, **0-2, 0-3, 0-4, 1-3**, **1-4**, **2-4** |
| Lateral | GV | 142 (18) | 147 (21) | 143 (14) | 139 (19) | 131 (18) | 0.196 | - |
| | GV' | 97 (14) | 99 (12) | 92 (12) | 93 (16) | 83 (14) | 0.032 | 0-4, 1-4 |
| | LBP/C | 6.53 (0.60) | 6.80 (0.61) | 6.94 (0.67) | 7.07 (0.60) | 6.81 (0.85) | <0.001 | 0-1, **0-2**, **0-3** |
| | $HI_{Lap}$ | 0.69 (0.02) | 0.69 (0.02) | 0.68 (0.02) | 0.69 (0.02) | 0.68 (0.02) | 0.235 | - |
| | $HI_{LBP}$ | 0.43 (0.01) | 0.43 (0.02) | 0.43 (0.01) | 0.43 (0.01) | 0.42 (0.01) | 0.689 | - |
| | $E_{Lap}$ | 7.08 (0.11) | 7.07 (0.11) | 7.07 (0.09) | 7.06 (0.10) | 7.03 (0.07) | 0.792 | - |
| | $E_{LBP}$ | 6.75 (0.06) | 6.77 (0.06) | 6.79 (0.05) | 6.81 (0.05) | 6.83 (0.03) | <0.001 | **0-2**, **0-3**, **0-4**, 1-3, 1-4 |

*Differences between groups using Fisher's LSD. Differences between groups using Bonferroni post-hoc test are bolded. GV = mean grayscale value, GV' = soft tissue subtracted from GV, $GV_{norm}$ = GV divided by the depth of the tibia, LBP/C = local binary patterns based contrast measure, $HI_{Lap}$ = homogeneity index from Laplacian-based image, $HI_{LBP}$ = homogeneity index from LBP-based image, $E_{Lap}$ = entropy from Laplacian-based image, and $E_{LBP}$ = entropy from LBP-based image.